

Design and analysis of a novel cable-driven haptic master device for planar grasping

Jadhao, K.S.; Lambert, Patrice; Bruckmann, T.; Herder, Just

DOI

[10.1007/978-3-319-61431-1_26](https://doi.org/10.1007/978-3-319-61431-1_26)

Publication date

2017

Document Version

Final published version

Published in

Cable-Driven Parallel Robots

Citation (APA)

Jadhao, K. S., Lambert, P., Bruckmann, T., & Herder, J. (2017). Design and analysis of a novel cable-driven haptic master device for planar grasping. In C. Gosselin, P. Cardou, T. Bruckmann, & A. Pott (Eds.), *Cable-Driven Parallel Robots: Proceedings of the Third International Conference on Cable-Driven Parallel Robots* (pp. 307-318). (Mechanisms and Machine Science; Vol. 53). Springer. https://doi.org/10.1007/978-3-319-61431-1_26

Important note

To cite this publication, please use the final published version (if applicable).
Please check the document version above.

Copyright

Other than for strictly personal use, it is not permitted to download, forward or distribute the text or part of it, without the consent of the author(s) and/or copyright holder(s), unless the work is under an open content license such as Creative Commons.

Takedown policy

Please contact us and provide details if you believe this document breaches copyrights.
We will remove access to the work immediately and investigate your claim.

Design and Analysis of a Novel Cable-Driven Haptic Master Device for Planar Grasping

Kashmira S. Jadhao¹, Patrice Lambert^{1(✉)}, Tobias Bruckmann²,
and Just L. Herder¹

¹ Delft University of Technology, Mekelweg 2, 2628 CD Delft, The Netherlands
jadhao.kashmira@gmail.com, {p.lambert, j.l.herder}@tudelft.nl

² University of Duisburg-Essen, Forsthausweg 2, 47057 Duisburg, Germany
tobias.bruckmann@uni-due.de

Abstract. This paper introduces a novel cable-driven planar haptic device with 4 DOF, six actuators, and two end-effectors, which can be used to provide planar motion and grasping capabilities. In this design, the rigid end-effector that is found in regular cable-driven robots is replaced by a configurable platform, i.e. a closed-loop that possess some internal DOF, which in the present case is made of cables in tension. Both the position and the configuration of the platform can be fully controlled through motors located on the frame of the device, offering a novel solution to provide grasping capabilities in parallel cable-driven mechanisms. After establishing the governing kinematics and statics relations, a workspace analysis of the novel mechanism is presented. Then, a proof-of-concept prototype has been developed in order to validate the kinematics. Finally, an optimization of the design parameters for maximal compactness of the system is presented. This design is expected to find applications in haptics technology due to its unique gripping mechanism and high structural stiffness architecture.

1 Introduction

In order to render realistic force feedbacks in impedance controlled haptic device, a device must possess a high mechanical bandwidth, such that the high-frequency content of the forces occurring during contact with stiff environment can be rendered properly. Parallel mechanisms [1] are often used now a days as haptic devices since they offer higher stiffness and lower inertia than comparable serial devices [2]. This is mainly due to the fact that all their motors are generally located on or near the base.

In some haptic applications, it is interesting to allow the operator to interact with the remote or virtual environment via multiple contact points, allowing the user to feel the shape and stiffness of the manipulated object. When grasping capabilities are needed, a conventional approach is to mount an additional grasper with a dedicated motor at the top of the parallel manipulator [3]. This however results in additional inertia and lower mechanical bandwidth, since mass is added at the point that is the furthest from the base.

Cable-driven parallel manipulators have also been used as haptic devices [4–6] because, aside from the advantages of rigid-link parallel manipulators, they can also offer a practically unlimited translational workspace and even lower inertia. However, adding an actuated haptic gripper to a cable-driven mechanisms would be more complicated due to the absence of rigid links to attach the power and communication wires, and would proportionally have a worst effect on the total inertia of the system.

In this paper, we propose a new type of cable-driven parallel mechanism, which offers planar motion and grasping capabilities with force feedback, while all the motors are located at the base. The innovative structure is based on the use of a multi end-effectors configurable platform [7], also formed by cables in tension, for which both the position and configuration can be fully controlled from the actuator at the base.

After a general presentation of the system in Sect. 2, the notation used and the geometric, kinematic and static analysis of the system are presented in Sect. 3 and their governing equations are summarized. Section 4 attains to the workspace definitions and analysis to describe the reach of the robot. Section 5 presents a demonstrator developed to validate the design and summarizes the obtained experimental results. Finally, Sect. 6 presents a way to optimize the system for maximum workspace to robot frame ratio.

2 System Description

This section introduces the novel cable-driven architecture on which the haptic device is based. The innovation in this architecture is in the use of a configurable platform made of two cables in tension which allows the interface to interact with the operator via two end-effectors (*EEs*), allowing grasping capabilities.

Figure 1 shows the schematic of the 4 DOF (two *EEs*, each having x and y translation capabilities) six actuators, cable-robot with the novel grasping mechanism. The red dots represent the location of the actuators on the robot frame, with cables connecting to the blue colored *EEs* and the rings (indicated as circles). The rings are allowed to slide along the two platform cables in order for the system to achieve equilibrium. While the cable lengths attached to the motors can vary with different positions of the *EEs*, the summarized lengths of the two cables between the two *EEs* are kept constant. The cable lengths between the *EEs* are based on the desired gripping distances, i.e. the desired minimum and maximum distance between the *EEs*. The gripping distances considered are 0.04 m to 0.10 m for ergonomic purposes. To enable these gripping distances, the cable lengths between the *EEs* are considered to be 0.105 m each which is the minimum requirement for a 0.10 m gripping distance and collisions avoidance. Although the minimum number of cable needed to fully control a 4 DOF mechanism is 5, an over-redundant design with six cables was preferred in order to achieve symmetry in the structure and more symmetry in the robot workspace and performance. Compared to the use of a dedicated grasping motor on the end-effector, enabling grasping capabilities from the coupled action of the motors located on the base reduces the inertia of the haptic device, improving the mechanical bandwidth of the mechanism.

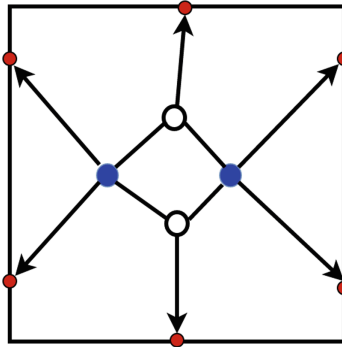


Fig. 1. Schematic of the 4 DOF, two end-effectors cable mechanism.

3 Geometric, Kinematic and Static Analysis

In this section, the kinematic relations between the end-effectors positions and the actuated cable lengths will be established based on the geometry of the architecture. The relations between the tensions in the actuated cables and the forces created at the end-effectors will also be introduced based on static equilibrium. We first introduce the notation and analysis of classical cable-driven robots and show how these concepts can be extended to a cable-driven robot with a configurable platform.

3.1 Modeling and Notation in Regular Cable-Driven Mechanisms

In case of planar robots, the orientation of each cable can be described with a unit vector \mathbf{d}_i along the cable i as

$$\mathbf{d}_i = \begin{bmatrix} d_{ix} \\ d_{iy} \end{bmatrix} \tag{1}$$

When tension f_i is applied, the cable i exerts a pure force $f_i \mathbf{d}_i$ on the end-effector. As a cable robot can function only when the cables are in tension, f_i always has to be positive. For a mechanism with a point-shaped end-effector, the total force applied on end-effector must be zero under static equilibrium. These conditions can be represented with the following system of equations:

$$\mathbf{A}^T \mathbf{f} + \mathbf{w} = \mathbf{0}, \quad f_i > 0 \tag{2}$$

where the structure matrix is represented by $\mathbf{A}^T = [\mathbf{d}_1 \ \mathbf{d}_2 \ \mathbf{d}_3 \ \mathbf{d}_4 \ \dots \ \mathbf{d}_m]$, the forces on the cables are summarized in $\mathbf{f} = [f_1 \ f_2 \ f_3 \ f_4 \ \dots \ f_m]^T$ and \mathbf{w} represents other external forces on the EE , like the gravity or other user defined forces.

The cable lengths (l_i) at each pose can be calculated by inverse kinematics. As explained by Tobias et al. in [12], it is possible to get satisfying force

values, for low velocities with applied low minimum force limits. However, with increasing velocities and accelerations the gripper starts to wobble due to slack cables. To avoid this, it is suggested to set appropriate upper (f_{max}) and lower (f_{min}) bounds on the system forces. For our system, forces were bounded by $f_{min} = 5$ N and $f_{max} = 100$ N. Since the mechanism exhibits force redundancy, multiple values of feasible forces for each robot pose are possible. In order to get at least one dimensional solution set for force distribution for a specific robot pose, we select the minimum Euclidean norm of vector \mathbf{f} as the applied forces. This optimal force solution set is computed for the desired system by using the MATLAB inbuilt optimization algorithm *fmincon*.

3.2 System Realization

Using the cable robot generic system equation as given in Eq. (2), the cable robot force equilibrium can be modeled.

$$\begin{bmatrix} d_{1x} & d_{2x} & d_{3x} \\ d_{1y} & d_{2y} & d_{3y} \end{bmatrix} \begin{bmatrix} f_1 \\ f_2 \\ f_3 \end{bmatrix} + \begin{bmatrix} 0 \\ 0 \end{bmatrix} = \begin{bmatrix} 0 \\ 0 \end{bmatrix} \quad (3)$$

Equation (3) represents the system equation for a three cables robot shown in Fig. 2(a). To extend this representation to our mechanism, we consider the complete architecture of the 4 DOF mechanism, as a collection of regular cable-driven mechanisms that are sharing some cables. For example, the system shown in Fig. 2(b) can be considered as two 3-cables mechanisms, sharing a common cable. This common cable introduces force constraints in the system. Forces f_3 and f_4 are equal in magnitude and opposite in directions as they represent the same cable. By concatenating the structure matrices for the two robots and adding an extra row to model the identical tension magnitudes in cables 3 & 4, the structure matrix for this arrangement is given by:

$$\begin{bmatrix} \mathbf{d}_1 & \mathbf{d}_2 & \mathbf{d}_3 & 0 & 0 & 0 \\ 0 & 0 & 0 & \mathbf{d}_4 & \mathbf{d}_5 & \mathbf{d}_6 \\ 0 & 0 & 1 & -1 & 0 & 0 \end{bmatrix} \begin{bmatrix} f_1 \\ f_2 \\ f_3 \\ f_4 \\ f_5 \\ f_6 \end{bmatrix} + \begin{bmatrix} 0 \\ 0 \\ 0 \\ 0 \\ 0 \\ 0 \end{bmatrix} = \begin{bmatrix} 0 \\ 0 \\ 0 \\ 0 \\ 0 \\ 0 \end{bmatrix} \quad (4)$$

Following this principle, the 4 DOF mechanism can be modeled as four mechanisms (2 nos. each of 3-cables & 4 cables mechanisms) sharing cables, as shown in Fig. 3(a). Besides the force constraints introduced by the shared cables on the system, the rings introduce additional constraints. The rings are not fixed entities like the *EEs* but are allowed to slide along the platform cables to achieve equilibrium when the *EEs* attain a particular configuration. The cables on the two sides of the rings are indeed the same cable. This results in the force equalities $f_5 = f_7$ and $f_{12} = f_{14}$. Concatenating the 4 mechanisms and adding these constraints due to the shared cables, the system equation for a 6 cable robot with 2 *EEs* is obtained.

Equation (5) represents the system equation of the 6 cable robot. In order to simulate this system of equations, it is necessary to know the positions of the rings and end-effectors a priori. The positions of the *EEs* are the input to inverse kinematics. If a ring can slide freely on a platform cable while keeping the cable in tension, it will trace the trajectory of an ellipse with the two *EEs* at the foci as shown in Fig. 4(a). In order to compute the positions of the rings, two hypothesis were laid down.

- (1) The rings will be positioned on the ellipse at a point which is at shortest distance from the pulley connected to that ring.
- (2) The line joining the pulley and the ring on the ellipse, aligns with the angle bisector of the angle formed by joining the two foci to the ring as in Fig. 4(b).

The second hypothesis comes from the fact that, at each junction (of rings/end-effectors), the forces are in equilibrium. Which means force f_6 in Fig. 3(a) is a resultant of the forces f_5 and f_7 . In theory, the resultant should be equal and opposite to force f_6 . The second hypothesis in fact validates the first hypothesis. Simulating the two conditions proved that the angle bisector described in hypothesis (2) is indeed the shortest distance discussed in hypothesis (1).

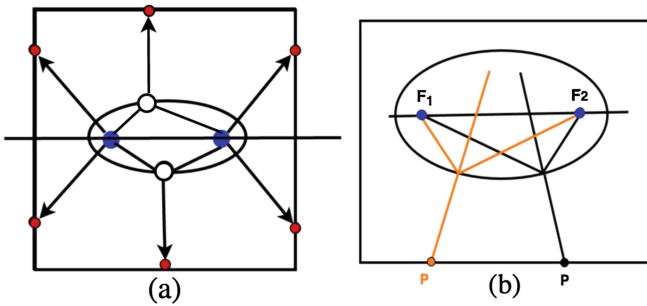


Fig. 4. System description (a) the ellipse concept with *EEs* at the foci and rings tracing the ellipse trajectory. (b) the shortest distance and angle bisector hypothesis, F are the ellipse foci.

4 Workspace Analysis

This section deals with the determination of workspace for the desired system [8,9,11]. The position of the mechanism is defined as the point at the mid distance between the two end-effectors. A point is considered a part of the workspace, if for its defined pose, all the cables have positive forces within the stated bounds [10]. To determine the workspace of the desired system, each point in the workspace is scanned to check and Eq. if all the required conditions are

satisfied. Figure 5(a) and (b) represent the robot workspace with an end-effector angle of 0° & 10° respectively. The grasping distance is 0.10 m and the design parameters as shown in Fig. 3(b) are $d_p = 0.15$ m and $L = W_f = 0.30$ m.

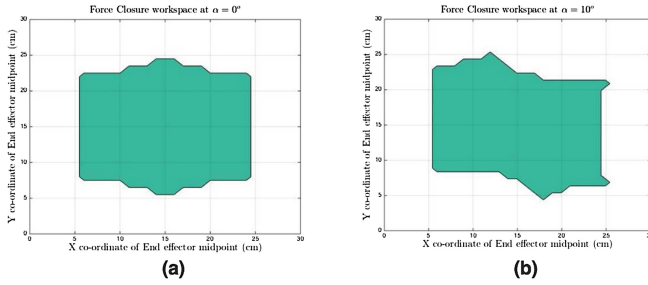


Fig. 5. Workspace with (a) *EEs* at 0° (b) *EEs* at 10° .

This being a haptic device, it is important for the operator that the workspace is easily conceivable. To deal with this problem, regular shaped workspace within the actual workspace was determined which involved computing the largest conceivable shape possible in the obtained contour. The new retrieved workspace will henceforth be referred as *Useful Workspace*, as shown in Fig. 6(a).

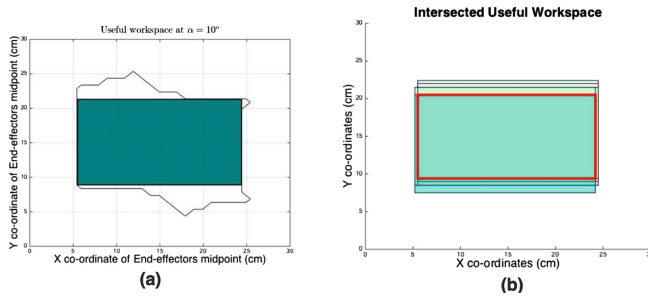


Fig. 6. (a) Useful workspace with *EEs* at 10° . (b) intersected Useful workspace area.

A point is a part of the translational workspace if all postures of robot are possible at that point i.e. at all defined gripper distances (distance between two *EEs*, g) and *EE* angles (represented by α in Fig. 3(b)) within certain ranges. It is observed that workspace size reduces with decreasing gripper distance and increasing magnitude of angle between the *EEs*. For the purpose of this paper, a gripper distance of 0.04 m to 0.10 m and an angular range for α of $\pm 10^\circ$ is considered. By varying geometric and design parameters d_p , W_f , L , α (as shown in Fig. 3(b)) and the gripping distance, different translational workspaces can be obtained.

An useful translation workspace for all gripper distances and different EE angles is computed as the intersection of useful workspaces for each gripping distance and EE angle values. As expected, this final workspace is much smaller than the initially computed useful workspace for individual gripping distances and EE angles. This whole process is depicted in Fig. 6(b).

5 Proof of Concept and Kinematic Validation

In order to validate the kinematic and static model of the novel architecture, a proof-of-concept demonstrator of the system was built and experiments were conducted for various tensions in the cables. This section illustrates the technical design of the robot architecture based on the proposed kinematic model. Task performance of the system is judged with positioning accuracy. The design is done keeping in mind haptics interface, which is considered as the final application of the system, and attention has been paid to ergonomics. These factors will govern the values of design parameters of the robot.

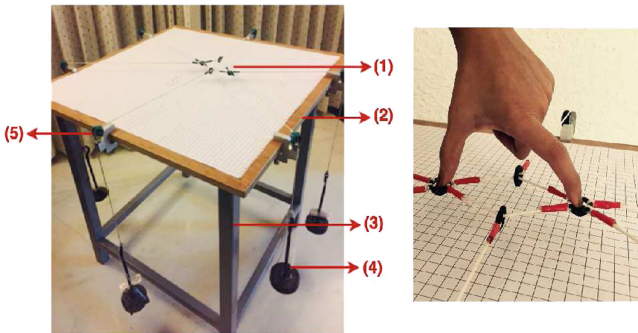


Fig. 7. Experimental set up (1) gripper (2) wooden plank, robot frame (3) table frame (4) weights and sandbags (5) pulley. Also shown: Gripping mechanism with two EE s and rings.

Figure 7(a) shows the experimental set up. It consists of a metallic table frame to hold the robot frame. A wooden plank of $0.75 \text{ m} \times 0.75 \text{ m}$ served as the robot frame. Six pulleys mounted on adjustable C-clamps were screwed to the frame. The distance between the two pulleys on the same edge of the frame was fixed at 0.19 m each from the center, while the single pulleys were positioned in the middle of the edge. Nylon wires with low elasticity were used as cables. For the gripper, two cups and two rings were used as shown in Fig. 7.

The 3D printed gripper cups have a dimension of $1.5 \times 10^{-2} \text{ m}$ diameter for a human finger to fit in. Gripper distances can be varied from $0.04 - 0.10 \text{ m}$, these figures are again ergonomically influenced, considering the minimum and maximum grasping possible for a human hand. For providing tensions in the

cables, discrete weights with sand bags for weight flexibility were hanged from the cables. A grid paper of 1×10^{-2} m x 1×10^{-2} m grids was stuck on the wooden plank for measurements.

While carrying out the experiment, it was important to take into account that the mechanical forces operating at the grippers, must be within a range that a human can exert. The considered force bounds for the system are 5–100 N which correspond to weights of 0.5 – 10 kg , operators can comfortably exert forces of any value in this range. Friction and other external forces on the system have not been accounted for in this design, however considering these forces will only alter the vector \mathbf{w} of the system Eq. (2), which will not be a difficult task.

The main objective for kinematic validation is to test if the proposed designed kinematic model works in a real set-up. Seven different positions of EEs , with different angles and gripping distances were given to the MATLAB code as inputs and the force values were noted. These positions were randomly selected and are presented in Table 1. Weights equivalent to these forces were hanged from the cables and the gripper was allowed to attain equilibrium. Once the gripper achieved stability, the positions of the EEs with angle and gripping distances were noted and compared with the simulated values. At every test point, the end-effector positions were marked with a pencil on the grid paper and the required measurements were taken from these markings after removing the EEs from the position. This helped in avoiding parallax to some extent. Table 1 shows a comparison between the simulated positions and the experimental positions, for the same cable tensions.

Table 1. Simulation & experimental data analysis

Simulated values			Experimental values			Error		
Angle (α) (deg)	Gripping dist. (g) (m)	Position (x,y) (m)	Angle (α) (deg)	Gripping dist. (g) (m)	Position (x,y) (m)	$\Delta \alpha$	Δg	($\Delta x, \Delta y$)
-10	0.06	(0.25, 0.26)	-11	0.064	(0.253, 0.27)	-1	0.4	(0.3, 1)
10	0.08	(0.58, 0.29)	9.2	0.83	(0.587, 0.293)	-0.8	0.3	(0.7, 0.3)
-5	0.07	(0.40, 0.40)	-5.4	0.072	(0.383, 0.39)	-0.4	0.2	(-1.7, -1)
-5	0.06	(0.29, 0.54)	-4.6	0.061	(0.292, 0.537)	0.4	0.1	(0.2, -0.3)
0	0.09	(0.20, 0.40)	0	0.096	(0.205, 40.05)	0	0.6	(0.5, 0.5)
5	0.08	(0.34, 0.34)	4.8	0.083	(0.33, 0.344)	-0.2	0.3	(-1, 0.4)
0	0.10	(0.47, 0.47)	0	0.095	(0.476, 0.47)	0	-0.5	(0.6, 0)

A number of factors affect the positioning accuracy of a system such as wear of parts, dimensional drifts, tolerances, assembly errors and limitations, friction, component manufacturing errors, measurement errors etc. These factors can explain the small deviations between the actual kinematic parameters and their nominal/experimentally obtained values.

6 Optimization

The workspace varies with size of the robot frame (length L and width W_f) and also with the distance between the two pulleys d_p as shown in Fig. 3(b). These three parameters namely L , W_f and d_p formed the design variables used for optimization of the useful workspace. Since the whole device can be scaled up or down, the optimization objective is defined as the ratio between area of the frame and area of the intersected useful workspace.

$$\text{Ratio} = \frac{\text{Area of frame}}{\text{Area of useful workspace}} \quad (6)$$

Table 2 briefly presents the optimization parameters, their roles and considered bounds.

Table 2. Optimization parameters

Parameter	Role	Notation	Bounds
Ratio	Objective function	Ratio	NA
Frame width	Design variable	W_f	10 to 20
Frame length	Design variable	L	10 to 20
Dist. between pulleys	Design variable	d_p	2.5 to W

Pattern Search and Grid Search optimization algorithms were used for this purpose and the optimizer was made to compute the workspace for angle values of -5° , 5° and 0° and gripping distances of 0.04 m – 0.08 m. These ranges are different than those considered for experimentation to aid optimization and reduce the simulation time. Grid Search algorithm performed a discrete crude search while a Pattern Search algorithm was used to refine the search. The entire workspace is scanned for feasible robot positions with a resolution of 0.01 m. The values for step size and resolution are considered to be discrete for the purpose of optimization as the complexity of the program and hence the computation time increases exponentially with increasing parameter and resolution precision.

Table 3. Optimization results for grid & pattern search algorithm

Parameter	Non-optimized value	Optimized value (grid search)	Optimized value (pattern search)
d_p (m)	0.10	0.14	0.16
L (m)	0.20	0.20	0.197
W_f (m)	0.20	0.20	0.197
Frame area (m ²)	0.04	0.04	0.039
Useful workspace (m ²)	93.5×10^{-4}	137.49×10^{-4}	137.49×10^{-4}
Ratio	4.28	2.91	2.83

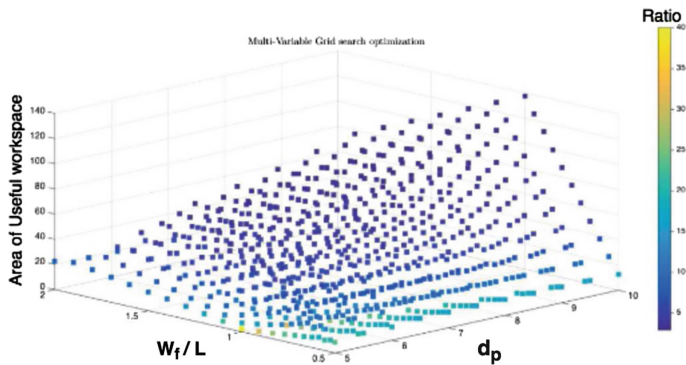


Fig. 8. Grid search plot.

Table 3 shows the optimization results for both the algorithms. Figure 8 show the variation of area of useful workspace with d and W_f/L .

Pattern Search algorithm was used to refine the search to cover the data skipped by Grid Search. However, there is not a significant difference between the results obtained in both the cases. This step to optimize the structure was done to get an idea about how the effective useful workspace changes with geometric parameters. Figure 8 shows how the workspace area varies with the chosen design parameters.

7 Conclusions

This paper presented a novel cable-driven master device for planar grasping for haptics interface. The need for a traditional gripper at the robot EE is eliminated by the unique gripper design with the two EEs and rings. Fixing the positions of the two EE , the position of the rings was geometrically computed for each pose of the robot. The wrench feasibility of the cable robot was investigated by $fmincon$ algorithm, such that all cables have positive tensions. The optimum values of cable forces were obtained which were set to fluctuate within pre-set minimum and maximum values of cable tension. The kinematic theory was validated through a working demonstrator. A comparative study of the results obtained experimentally and through simulations was done to support the design validation. Finally, a design optimization was carried out to maximize the workspace of the device for a given frame dimension. This design is expected to find applications in haptics technology due to its unique gripping mechanism and light and sturdy architecture.

References

1. Jean-Pierre Merlet. *Parallel Robots*, vol. 53 (2013)
2. Pandilov, Z., Dukovski, V.: Comparison of the characteristics between serial and parallel robots. *Fascicule 1*, 2067–3809 (2014)
3. Tobergte, A., Helmer, et al.: The sigma. 7 haptic interface for MiroSurge: a new bi-manual surgical console. In: 2011 IEEE/RSJ International Conference on Intelligent Robots and Systems (IROS), pp. 3023–3030. IEEE (2014)
4. Robert, L., Williams, I.I.: Cable-suspended haptic interface. *Int. J. Virtual Reality* **3**(3), 13–21 (1998)
5. Gosselin, C.: Cable-driven parallel mechanisms: state of the art and perspectives. *Mech. Eng. Rev.* **1**(1), DSM0004 (2014)
6. Tobias, B., Lars, M., Thorsten, B., Manfred, H., Dieter, S.: Design approaches for wire robots. *ASME Conference Proceedings* (49040), pp. 25–34 (2009)
7. Lambert, P.: Parallel robots with configurable platforms: fundamental aspects of a new class of robotic architectures. *Proc. Inst. Mech. Eng. Part C J. Mech. Eng. Sci.* **230**(3), 463–472 (2016)
8. Ghasemi, A., Eghtesad, M., Farid, M.: Workspace analysis of planar and spatial redundant cable robots. In: *Proceedings of the American Control Conference*, pp. 2389–2394 (2008)
9. Berti, A., Merlet, J.P., Carricato, M.: Workspace analysis of redundant cable-suspended parallel robots. *Mech. Mach. Sci.* **32**, 41–53 (2015)
10. Bosscher, P., Riechel, A.T., Ebert-Uphoff, I.: Wrench-feasible workspace generation for cable-driven robots. *IEEE Trans. Robot.* **22**(5), 890–902 (2006)
11. Lolei, A.Z. Aref, M.M., Taghirad, H.D.: Wrench feasible workspace analysis of cable-driven parallel manipulators using LMI approach. In: *IEEE/ASME International Conference on Advanced Intelligent Mechatronics, AIM*, pp. 1034–1039 (2009)
12. Bruckmann, T., Pott, A., Franitza, D., Hiller, M.: A modular controller for redundantly actuated tendon-based stewart platforms. In: *EuCoMes, Obergurgl, Austria* (2006)